ELSEVIER

International Journal of Mass Spectrometry 219 (2002) 515–523

International Journal of Mass Spectrometry

www.elsevier.com/locate/ijms

Irradiation effects in MALDI and surface modifications Part I: Sinapinic acid monocrystals

I. Fournier, J.C. Tabet, G. Bolbach*

Laboratoire de Chimie Structurale Organique et Biologique, Université P&M CURIE, CNRS–UMR 7613, Boîte 45, 4 Place Jussieu 75252, Paris Cedex 05, France

Received 25 January 2002; accepted 19 April 2002

Dedicated to Dr. Yannik Hoppilliard on the occasion of her 60th birthday.

Abstract

The origin of the irradiation effect on the ion production in MALDI processes, using large sinapinic acid crystal, was studied in conjunction with the surface modifications. Characterization of the crystal irradiated surfaces by a commercial N_2 laser, from which ion production was quenched at the normal laser threshold energy, with scanning electron microscopy and light microscopy show very dramatic modifications of the surface structure. Three main regions with different morphologies were observed. A region with small craters in the center of the spot, a strong perturbed contiguous area with hill–valley patterns and a bead periodical structure extending up to the rim of the spot. Periodical bead structure mainly is responsible for the disappearance of ion production. Theses structures are eliminated after one or two shots at high energy. The analysis of the uppermost layers of the irradiated and non-irradiated surfaces, performed by chemical ionization with quadrupole mass analyzer, indicates that the matrix, at surface, yields mainly to decarboxylated sinapinic acid. The physical properties of the modified matrix can be responsible for the structural changes on the irradiated target and the vanishing of ion production. (Int J Mass Spectrom 219 (2002) 515–523)

Keywords: MALDI; Irradiation effects; Ablation process; Ionization processes; Mechanisms

1. Introduction

Although matrix-assisted laser desorption/ionization (MALDI) [1,2] is now a powerful tool in analysis and is extensively used especially in bioanalysis, ablation/ionizations processes are still not well understood. Great instrumental developments have been realized the last 10 years but are still lacking a better understanding of the chemico-physical phenomena involved in MALDI. However, several studies have been dedicated to fundamental processes and different desorption and/or ionization models have been proposed. Nevertheless, some striking features remain difficult to interpret even in the frame of the models. For example, decreasing of signal intensity during a MALDI experiment is currently observed.

In a previous paper, we described laser irradiation effects on sinapinic acid large crystals [1]. At the laser energy of the ion production threshold (matrix and peptide), the ion peak intensity decays with the number of laser shots and drops to zero after typically 120 laser shots. On the same spot, the ion signal cannot be recovered at the energy threshold at any time thereafter. However, one or two laser shots at high

* Corresponding author. E-mail: bolbach@ccr.jussieu.fr

1387-3806/02/$ – see front matter
PII S1387-3806(02)00704-2

energy on the same spot allow to retrieve ion signal at the normal laser energy threshold. Sequences of threshold irradiations followed by one or two high energy irradiation can be performed indicated a phenomena of hysteresis in the ion production [3]. This behavior only depends upon the nature of the matrix and not on the presence of analyte. It is independent of the hydrophobic or hydrophilic nature of the crystal surface. Substituted cinnamic acids (sinapinic acid, α-cyano-4-hydroxycinnamic acid [3]) exhibit this property but not 2,5-dihydroxybenzoic acid [4]. In a conventional MALDI experiment using the dried droplet method, this difference can be also noted. For substituted cinnamic acid and at the laser energy threshold, the ion signal vanishes after a certain number of exposures of a given spot on the sample.

The aim of this present study was to determine the origin of this effect by studying the modifications in the structure and composition of the irradiated matrix crystal surface. When most of the attention was paid on the material ablated by the laser pulses (mainly ion production), this paper will focus on the target energy relaxation after ablation and its consequence on further ion production.

2. Experimental

2.1. Large crystal growing

Sinapinic acid (*trans*-3,5-dimethoxy-4-hydroxycinnamic acid) was purchased from Aldrich and used without further purification. Large sinapinic acid crystals doped or not with various peptides (substance P, bovine insulin or horse apomyoglobin) were grown as previously described [3]. Crystals were glued on the gold surface of the sample holder by depositing a small drop of water at the boundary between the crystal and the metal surface.

2.2. Laser irradiation and MALDI-TOF mass spectrometry

Crystals were irradiated by the N_2 laser (λ = 337 nm, 3 ns pulse duration, repetition rate 2 Hz, VSL 337 ND, Laser Science Inc.) equipping the Voyager Elite MALDI time-of-flight mass spectrometer (PerSeptive Biosystems, Boston, MA). The angle of incidence was 45°. A video monitor allowed to display a real-time video image of the sample spot during laser irradiation and to follow the macroscopic surface modifications through reflectance changes. The laser pulse energy, adjusted with a circular neutral filter, was measured using an energy meter (RJ7100 Laser Precision Corp.).

MALDI mass spectra were performed in the linear mode using the ion wire guide and a high mass detector.

2.3. Scanning electron microscopy

The characterization of the irradiated samples was performed on a LEICA 440 directly on the sample holder used for laser irradiation without any manipulation of the sample. For the thickest crystals, a gold layer of 150 Å was deposited to avoid charge effects.

2.4. Mass spectrometry studies of surface chemical modifications

As thin as possible a surface layer (∼40 μm) was cleaved off the irradiated crystal and dissolved in acetonitrile/water 4:1 (v/v). A few microliters were deposited on the tungsten filament of the direct introduction probe for PICI experiments. A triple quadrupole mass spectrometer (Nermag R 30-10, Rueil-Malmaison) was used with a modified high pressure source. Ammonia was the chosen gas phase reagent within a pressure of 0.1 Torr.

3. Results

3.1. Surface modification by irradiation at the laser energy threshold

Hydrophobic surfaces $(1\,0\,\bar{3})$ of sinapinic crystals irradiated by 256 laser shots at the energy threshold

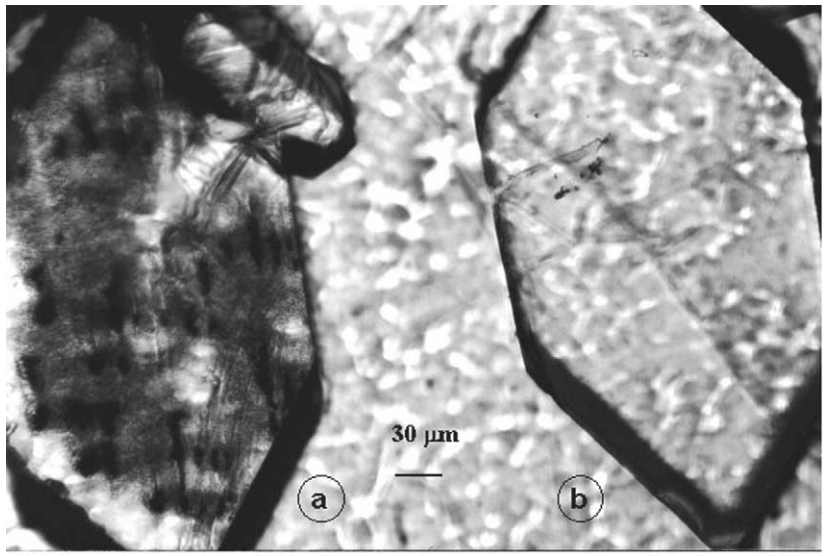

Fig. 1. Light microscope photo of the hydrophobic surfaces of sinapinic acid crystal: (a) after irradiation of 12 different spots of the surface by 256 laser shots at the energy threshold for ion production and (b) without irradiation. The sample was illuminated by a visible light source with a blue filter and reflected light was analyzed by the microscope.

(2.3 μJ/pulse) for ion production have shown important changes of reflectivity. The irradiated spots appeared, at naked eye, darker than a non-irradiated surface. This is illustrated by the light microscopy images (Fig. 1) of an hydrophobic surface irradiated on different spots (Fig. 1a) compared to a non-irradiated surface (Fig. 1b). From the surface in Fig. 1a, no ion production can be detected at the normal energy threshold. A typical irradiated spot showed a large dark area and inside two smaller but darker areas. An irradiated single spot is shown on the SEM image (Fig. 2a). Details of the spot clearly show three

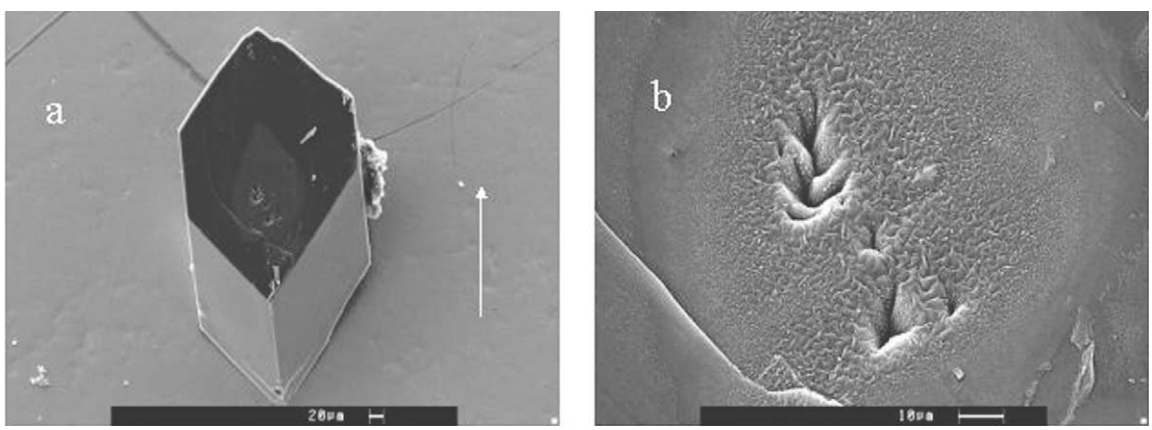

Fig. 2. Scanning electron micrograph of the hydrophobic surface of a sinapinic acid crystal irradiated by 3936 laser shots at the energy threshold (2.3 μJ/pulse): (a) a view of the entire crystal and the irradiated area. The arrow indicates the projection of the incidence direction; (b) view of the craters; (c) view of the vicinity of one crater; (d) view of the region between the crater region and the rim of the irradiated spot showing the bead morphology; and (e) view of the rim of the irradiated spot showing recondensation products.

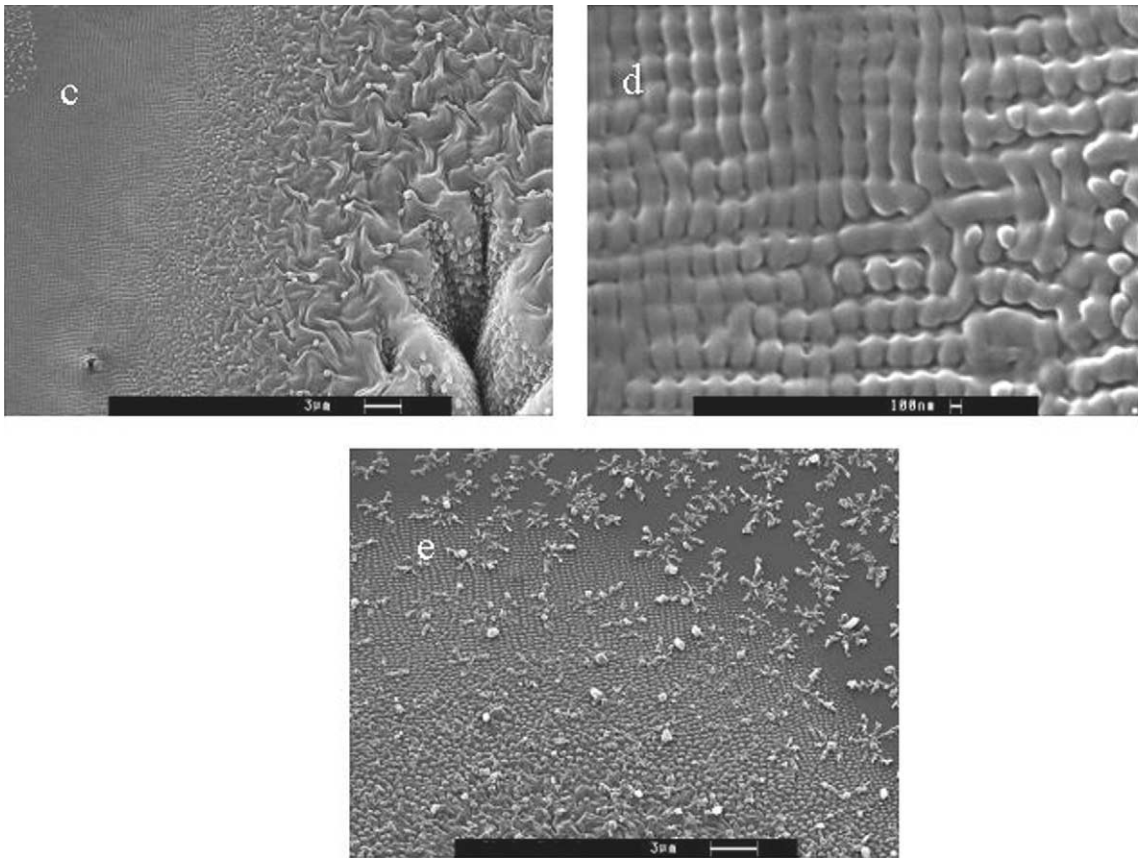

Fig. 2. (*Continued*).

main regions characterized by different morphologies. A region where ablation clearly occurred with mainly two small craters as shown in Fig. 2b near the center of the irradiated spot. A second region, contiguous to the previous one, showing a strong perturbed area of high roughness with hill–valley patterns (Fig. 2c). The third region extending up to the rim of the spot exhibits a periodical structure similar to beads (∼1000–2000 Å in diameter) joined end to end (Fig. 2d). This structure covers about 55% of the total area of the spot. Behind the rim and all around of the irradiated area, deposits are observed (see the left-up corner in Fig. 2c and e), likely resulting from a recondensation of ablated products [4].

Similar results were obtained for irradiations of hydrophilic surfaces near the energy threshold of ion production (data not shown). It should be noted that the three different morphologies described above appear when the number of shots corresponding to the complete disappearance of ion production is achieved. Any further exposures modify only the inner surface of the craters. Fig. 3a and b show the structure of the crater after irradiation at the threshold energy with 256 and 1280 laser shots, respectively. Extended irradiation strongly modifies the surface of the crater. In particular, the surface of the crater, very smooth at smaller number of exposures, gets covered by a bead layer after extended irradiation (Fig. 3b). The beads have a similar diameter (∼1000–2000 Å) to the ones in the third region previously described. In addition, the base of the crater is not plane. All these observations give evidence of strong local effects. In particular, the

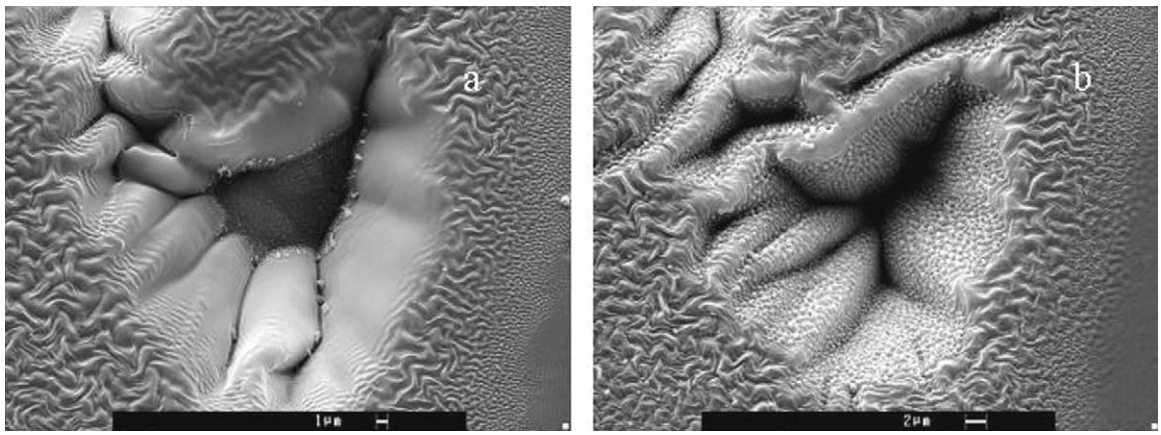

Fig. 3. Scanning electron micrograph of a hydrophilic surface of a sinapinic acid crystal: detail of the crater (a) after irradiation by 256 laser shots and (b) after irradiation by 1280 laser shots (laser energy: 2.5 μJ/pulse).

surface of the crater formed by 256 laser shots is modified by further irradiation but the diameter of the crater is not altered indicating that ablation, as well as ion production, is not effective beyond this irradiation.

Fig. 4 shows the crater resulting from the irradiation of a hydrophilic crystal surface by 24 laser shots at higher energy (8.6 μJ). Two laser shots at this energy allow to recover ion signal for irradiation at threshold. The surface at the base of the

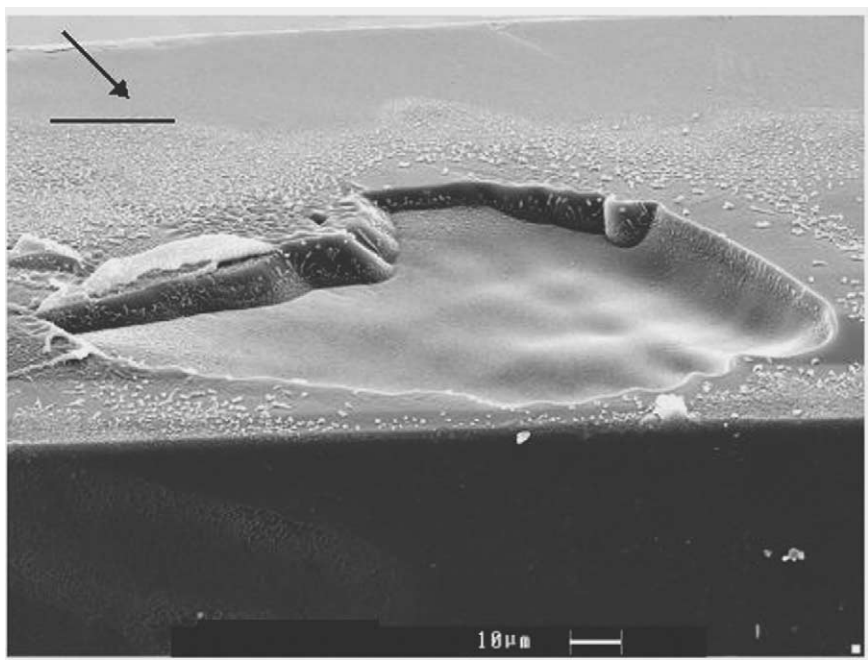

Fig. 4. Scanning electron micrograph of the hydrophilic surface of a sinapinic acid crystal irradiated by 24 laser shots at high laser energy (8.6 μJ/pulse). The arrow indicates the direction of the laser incidence.

crater is smooth and the previous structures above mentioned are no more observed. The shape of the crater (∼100 μm × 150 μm) is similar to that of the irradiated spot at energy threshold (Fig. 1) and its depth is ∼6 μm. At this laser energy, the recondensation of ablated products is much more pronounced.

A possible explanation for ion production vanishing at the energy threshold can be related to the change of surface structure. The formation of three structures involves a dramatic increase of the surface roughness leading to important changes in local beam penetration depth, reflectivity and shadowing effect are expected. As the main structure of the irradiated spot is the periodic beads one, the beads diameter (∼1000 Å) allows to estimate that the roughness is increased by a factor of 1.5. A spot, previously irradiated with successive pulses at energy threshold until ion detection ceased, was then irradiated with a pulse of increased energy. We found that ion production start again when the

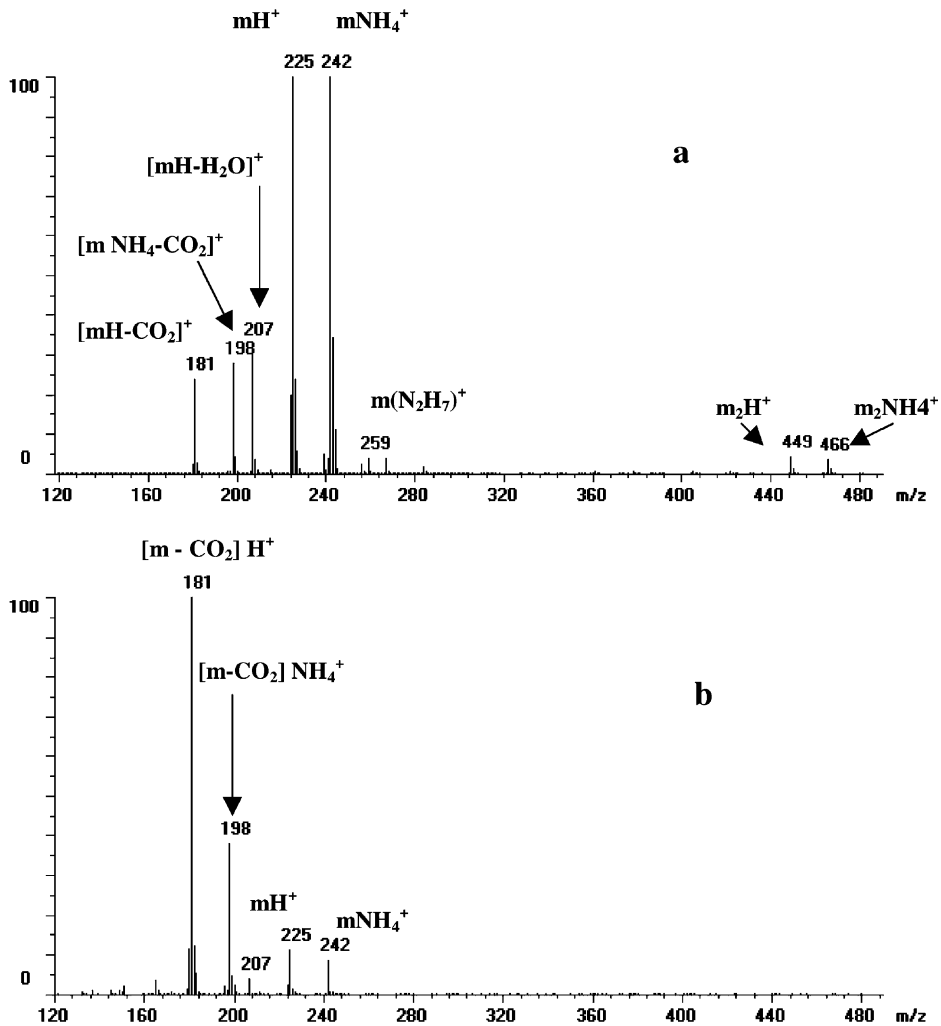

Fig. 5. Ammonia chemical ionization mass spectra (positive mode) of a (a) non-irradiated sinapinic acid crystal surface slice and (b) irradiated slice by 256 laser shots at different spots at the energy threshold for ion production (see text).

laser energy is higher or equal to 1.6-fold the threshold energy.

3.2. Chemical modification of the irradiated surface

During irradiation experiments at the energy threshold no peculiar feature was detected in the MALDI mass spectra. Apparition of new ion species or variations in the relative intensity of usual ions has not been observed in the mass range involving the matrix parent (monomer and multimer) and fragment ions. In particular, no truxillic acid derivatives were found [5–9]. We tried to study if chemical modifications of the irradiated surface at the energy threshold were involved in the new macroscopic structures mentioned above. For this purpose, we only used the irradiated hydrophobic sinapinic acid surfaces since they can be easily cleaved [3,17]. Such surfaces were irradiated at different spots so that the entire crystal surface gave a change of reflectivity (see above and Fig. 1a). Using a scalpel, the finest cut of the irradiated surface was then operated and typically a material slice of 40 μm of thickness beneath the surface was extracted. After dissolution in acetonitrile/water 1:4 (v/v), the material was first studied in MALDI by depositing 1 μL of the solution on the target holder or mixing 1 μL of the solution with the matrix 2,5-DHB. No new ion specie was detected. In particular, the analysis of 1 μL of the solution leads to the same MALDI mass spectrum of sinapinic acid than that of a classical dried droplet deposit or non-irradiated large crystals. It should be noted that in the extracted slice of the crystal surface (∼40 μm), the real perturbed region (probably, a few thousands of Å) likely represents a minor contribution.

Further analysis of the cleaved material was then performed using positive ion chemical ionization with the NH_4^+/NH_3 system (PICI–NH_3). The solution was deposited on a tungsten filament without heating. Fig. 5 shows the mass spectra of the irradiated surface slice (Fig. 5b) compared to a non-irradiated one (Fig. 5a) recorded in the same high pressure conditions. The major ions for the non-irradiated surface slice correspond to MH^+, MNH_4^+ and their decarboxylated forms (Fig. 5a). Very dramatic changes were observed for the irradiated slices with two major components corresponding to the protonated decarboxylated forms $[M - CO_2 + H]^+$ and their ammonium adduct forms $[M - CO_2 + NH_4]^+$. The other ions, protonated molecules and ammonium adduct molecules as well as the fragment corresponding to water loss of the protonated molecule remained in the same proportion as those in the non-irradiated slice. The experiments on the irradiated and non-irradiated slices being done strictly in the same conditions, these results suggest that in the irradiated slice a (partial) decarboxylation of the matrix molecules has occurred. This finding has to be compared to the observation by Goldschmidt et al. [9] of CO_2 emission during the UV irradiation under vacuum conditions of cinnamic derivatives including the sinapinic acid.

4. Discussion

Irradiation of sinapinic acid crystals using laser energy near the threshold of ion production shows dramatic changes in the morphology of the hydrophobic and hydrophilic surfaces. Three main morphologies have been observed and are likely related to the non-uniform spatial energy distribution of the nitrogen laser. However, changes in the surface morphology were also found in the irradiation effects of 2,5-DHB single crystals using a flat-top UV laser [10]. At the threshold fluence for ion production, cone structures pointed towards the direction of the laser beam and known as “Trulli” structures were observed [10]. These authors also mentioned that extended irradiation at higher fluences produced ablation craters without specific morphology.

The quenching of ion production is likely connected to chemical modification at the crystal surface through the decarboxylation, partial or total, of matrix molecules in the irradiated area. It should be noted that the relative abundance of protonated decarboxylated form of matrix molecules was not found to increase as a function of the laser exposure in the direct MALDI mass spectrum. Thus, matrix decarboxylation at the surface of the sample is not a process

directly involved in ablation/ionization mechanisms. In addition, the results obtained by Goldschmidt et al. [9] on the CO_2 emission from sinapinic acid target under extended UV laser irradiation is in good agreement with our result on the decarboxylation of such a matrix. One should note that a CO_2 emission was also found as ablation product of irradiated polymers such as PMMA and PET [11].

The origin of these tree main morphologies is not obvious. From the literature, most of the studies on the irradiation effects were devoted to covalent material (semiconductor, metal, composites, etc.) using much higher laser fluences and to polymers. Similar "bead structure" have already been observed after laser irradiation of silicon surfaces [12], nitrogen laser irradiation of polyimide [13], XeCl excimer laser ablation of cobalt cemented tungsten carbide samples [14] and after clusters impact on Au metal surface [15]. In all these cases and according to the authors, the surface after extended irradiation looks like a melt-induced structure. This conclusion is also supported by the ablation of polymers such as PMMA with 193 nm laser pulse [11]. In the case of sinapinic acid crystal surfaces similar effects can be assumed. A phase transformation due to the decarboxylation of matrix molecules at surface and in depth of material could be also due to a rapid heating of the surface by the photon absorption and internal conversion or by heating and pressure wave transport near the surface. It should be noted that CO_2 emission was also found by irradiating $CaCO_3$ crystal with IR laser [16].

The decarboxylation of carboxylic acid after heating is a well-known phenomenon in chemistry [14]. A consequence of the matrix decarboxylation is the dramatic change of interaction between molecules in the crystal. The carboxylic groups, as well as the hydroxyl group, participate to the cohesion binding of the non-covalent crystal, through hydrogen bonds [17]. A partial or total decarboxylation involving a partial disappearance of the local order in the crystal could also modified the material surface tension and other physical parameters (volatility, melting point, etc.). The globular form of the bead morphology could result from such effects (Fig. 2d), in particular, the surface tension modification, during the natural cooling of the surface by internal energy relaxation and the new structure would be "frozen" [18]. It should be noted that the non-uniform spatial energy of the nitrogen laser expected in these experiments give a rather large homogeneous bead region. This can give likely evidence of lateral heating transport. Also, a lateral matter transport due to a "piston" mechanism [12] can be responsible for the ejection of melt material and its recondensation beyond the rim of the irradiated spot.

Matrix decarboxylation at the surface of the target likely involves the change of UV absorption. General trends, in solution, indicate that a shift of 30 nm towards the higher wavelengths would be expected for each additional conjugated double bond of such aromatic compound [19]. Thus, matrix decarboxylation would involve a shift of ∼30 nm of the absorption band toward the shorter wavelengths with respect to unmodified sinapinic acid. Taking into account the matrix absorption studied by Allwood et al. [20], such a shift would give a decrease of the absorption coefficient by typically a factor of 2 for sinapinic acid. This decrease would be sufficient to explain the ion production quenching.

Matrix ablation/ionization and decarboxylation of matrix molecules at surface appear as different phenomena in MALDI during the extended irradiation at the energy threshold of a same spot. Ablation/ionization is a fast phenomenon occurring in a time scale of the laser pulse duration, and is mainly driven by the absorption of UV beam. Decarboxylation can be driven by slower energy relaxation processes similar to heating and it appears as the waste product of the irradiation. The gradual increase of decarboxylated matrix molecules concentration at surface and or just underneath with the exposures gradually decreases the UV absorption until the fluence at any region of the surface becomes lower than the fluence threshold and ablation/ionization is then quenched. Such accumulating effects were extensively studied in the irradiation of polymers [21,22]. In particular, the etching of PMMA by a 193 nm laser beam starts only if a minimum number of pulses ("incubation") irradiated the target [21], the absorption

coefficient being dependent on this degree of incubation [22].

At high laser energy, however, ablation is the major effect since the surface roughness strongly decreases (see above and Fig. 4). The strong ablation probably ejects the region containing the decarboxylated matrix molecules, if they are formed. Alternatively and more likely, the energy relaxation in surface is very fast and the decarboxylation process does not occur. At laser energy close to the threshold of ion production, the matrix decarboxylation could prevent the ablation and the ion formation especially in the bead region through a decreasing of local absorption. The decarboxylation process in the region around the craters (Fig. 2c) would compete gradually with ablation with increasing laser exposures. This would be also verified for the crater region (Fig. 3b) for which bead morphology was found after extended irradiation at the threshold energy.

5. Conclusion

The physical and chemical processes in MALDI appear very complex since they involved not only ablation and ion production but also strong changes in morphology of the irradiated sinapinic acid surface. Physical and chemical effects through matrix decarboxylation are involved in the surface morphologies and this change of surface composition influences the surface roughness and presumably the photon absorption. Matrix decarboxylation is probably due to pyrolysis connected to slow energy relaxation at the matrix surface after (or concomitant) to the ablation process. In the extended irradiation at the energy threshold, the matrix decarboxylation is likely at the origin of the gradually decreases of the ion production through the UV absorption decrease. The results presented here on the sinapinic acid can be also extended to other substituted cinnamic acid matrices, in particular for α-cyano-4-hydroxycinnamic acid [23] for which similar irradiation effects are observed.

New experiments will be needed to know if the CO_2 release, associated to the matrix decarboxylation during or just after the laser irradiation, could play a role in the ablation process and in the formation of the supersonic beam and plume.

References

[1] M. Karas, F. Hillenkamp, Anal. Chem. 60 (1988) 2299.
[2] K. Tanaka, Y. Ido, S. Akita, Y. Yoshida, T. Yoshida, Rapid. Commun. Mass Spectrom. 2 (1988) 151.
[3] I. Fournier, R.C. Beavis, J.C. Blais, J.C. Tabet, G. Bolbach, Int. J. Mass Spectrom. Ion Process. 169/170 (1997) 19.
[4] M. Schürenberg, T. Schulz, K. Dreisewerd, F. Hillenkamp, Rapid Commun. Mass Spectrom. 10 (1996) 1873.
[5] M.D. Cohen, G.M.J. Schmidt, J. Chem. Soc. 384 (1964) 1996.
[6] M.D. Cohen, G.M.J. Schmidt, F.I. Sonntag, J. Chem. Soc. 384 (1964) 2000.
[7] G.M.J. Schmidt, J. Chem. Soc. 384 (1964) 2014.
[8] J. Bregman, K. Osaki, G.M.J. Schmidt, F.I. Sonntag, J. Chem. Soc. 384 (1964) 2014.
[9] R. Goldschmidt, R. King, K. Balasanmugam, J. Scable, K.G. Ovens, in: Proceedings of the 40th ASMS Conference on Mass Spectrometry and Allied Topics, Washington, DC, 1992, p. 374.
[10] J. Kampmeier, K. Dreisewerd, M. Schürenberg, K. Strupat, Int. J. Mass Spectrom. Ion Process. 169/170 (1997) 31.
[11] R. Srinivasan, B. Braren, Chem. Rev. 89 (1989) 1303.
[12] M. von Allmen, A. Blatter, Laser-Beam Interactions with Materials, 2nd Edition, Springer, Berlin, 1994.
[13] Z. Qin, J. Zhang, H. Zhou, Y. Song, T. He, Nucl. Instrum. Meth. B 170 (2000) 406.
[14] T. Li, Q. Lou, J. Dong, Y. Wei, J. Liu, Appl. Surf. Sci. 172 (2001) 51.
[15] I. Yamada, J. Matsuo, N. Toyoda, A. Kirkpatrick, Mater. Sci. Eng. R 34 (2001) 231.
[16] H.K. Park, R.F. Haglund, Appl. Phys. A 64 (1997) 431.
[17] R.C. Beavis, J.N. Bridson, J. Phys. D 26 (1993) 442.
[18] T.R. Anthony, H.E. Cline, J. Appl. Phys. 48 (1977) 3888.
[19] Pretsch–Clerc–Seibl–Simon (Ed.), Table of Spectral Data for Structure Determination of Organic Compounds, Springer, Berlin, 2nd Edition, 1989.
[20] D.A. Allwood, R.W. Dreyfus, I.K. Perera, P.E. Dyer, Rapid Commun. Mass Spectrom. 10 (1996) 1575.
[21] E. Sutcliffe, R. Srinivasan, J. Appl. Phys. 60 (1986) 3315.
[22] S. Küper, M. Stuke, Appl. Phys. B 44 (1987) 199.
[23] I. Fournier, M. Glückmann, M. Karas, in: Proceedings of the 49th ASMS Conference on Mass Spectrometry and Allied Topics, Chicago, 2001.